Evaluation of CAM Track 5 Ice Microphysics Using In Situ Measurements and Satellite Remote Sensing

David L. Mitchell and Subhashree Mishra
Desert Research Institute, Reno, Nevada

Philip J. Rasch
PNNL, Richland, Washington

R. Paul Lawson
SPEC, Inc., Boulder, Colorado

Objective 1: Beginning with measurement derived ice particle size distribution (PSD) schemes that depend on temperature and IWC, make them consistent with thermal radiances measured from satellites. This is expected to correct for ice artifacts produced by shattering of ice particles on the probe inlets.

Objective 2: Compare these corrected PSD and associated PSD fallspeeds (V) and effective diameters (D_e) with PSD, V and D_e from CAM Track 5 simulations.

How Photon Tunneling Can be Used to Remotely Detect Small Ice Crystals in Cirrus

Photon Tunneling is the process by which radiation beyond the physical cross-section of a particle is either absorbed or scattered outside the forward diffraction peak. Tunneling is strongest when:

1) **Effective size and wavelength are comparable**

2) **Particle shape is spherical or quasi-spherical**

3) **The real refractive index is relatively large**

Therefore tunneling contributions at terrestrial wavelengths are greatest for smallest (D < 60 μm) ice crystals. To detect the tunneling signal is to detect small ice crystals.

Size dependence of tunneling for single ice crystals

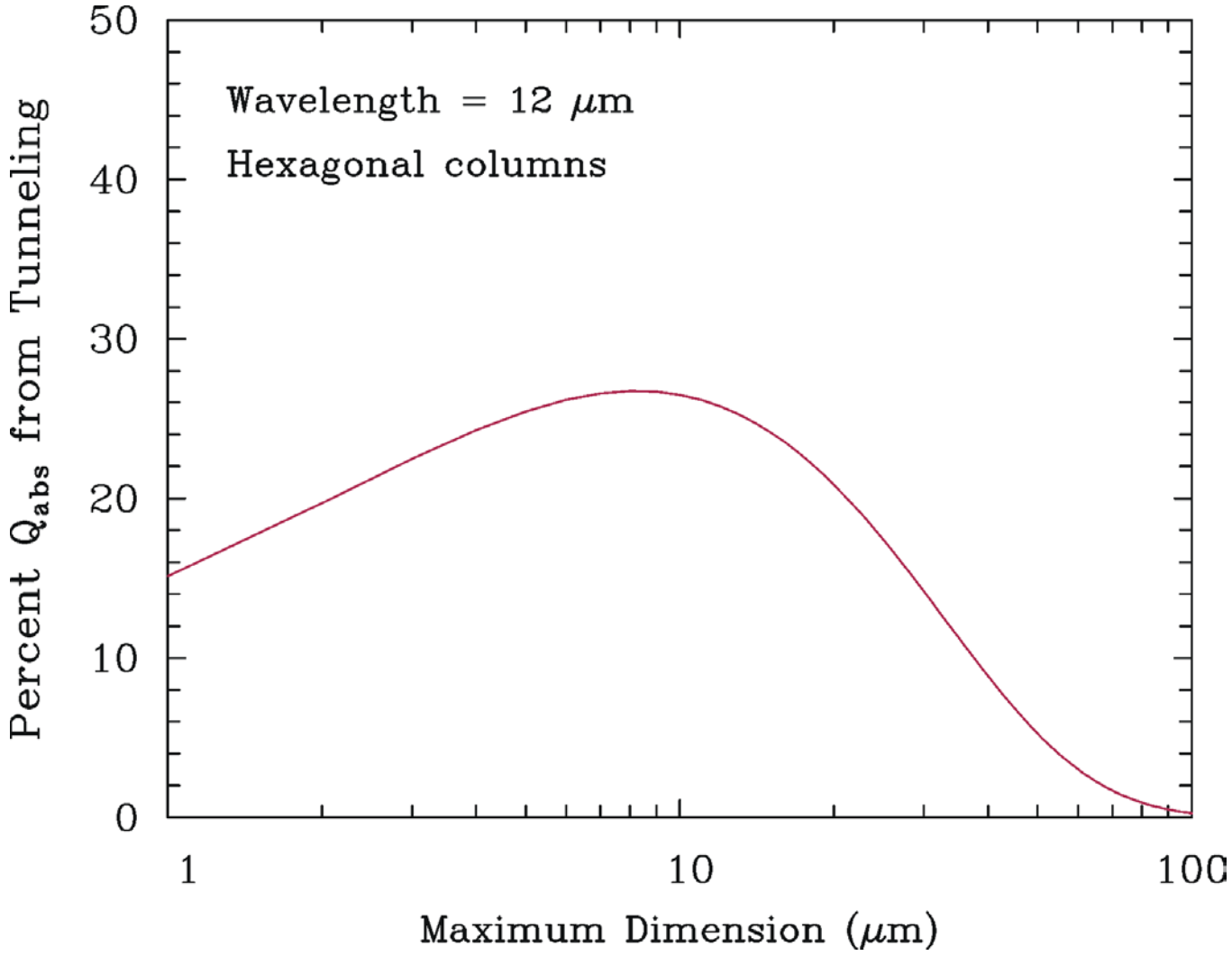

Example of ice particle size distribution (PSD) scheme for evaluating potential tunneling contributions

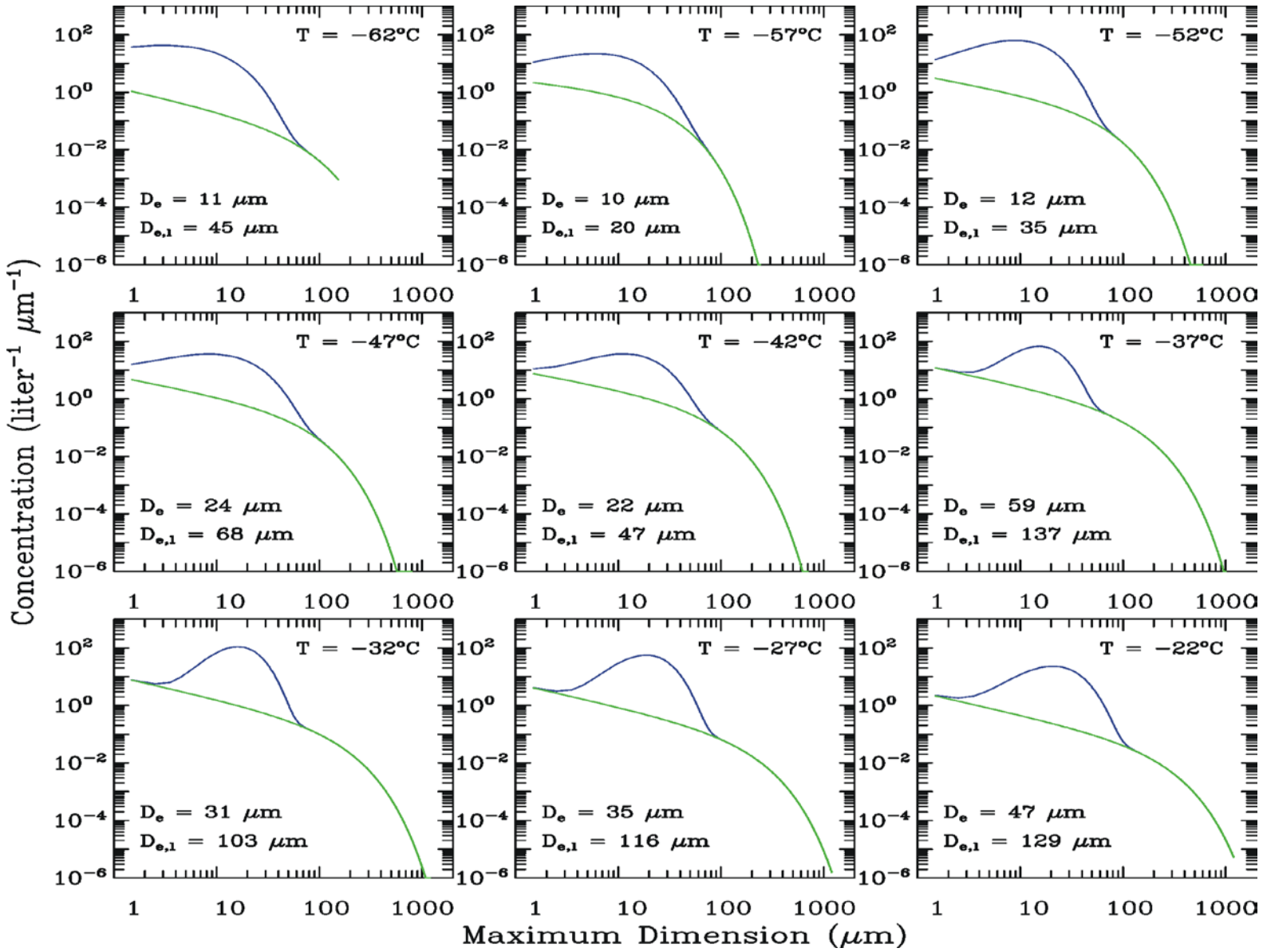

Size and wavelength dependence of tunneling

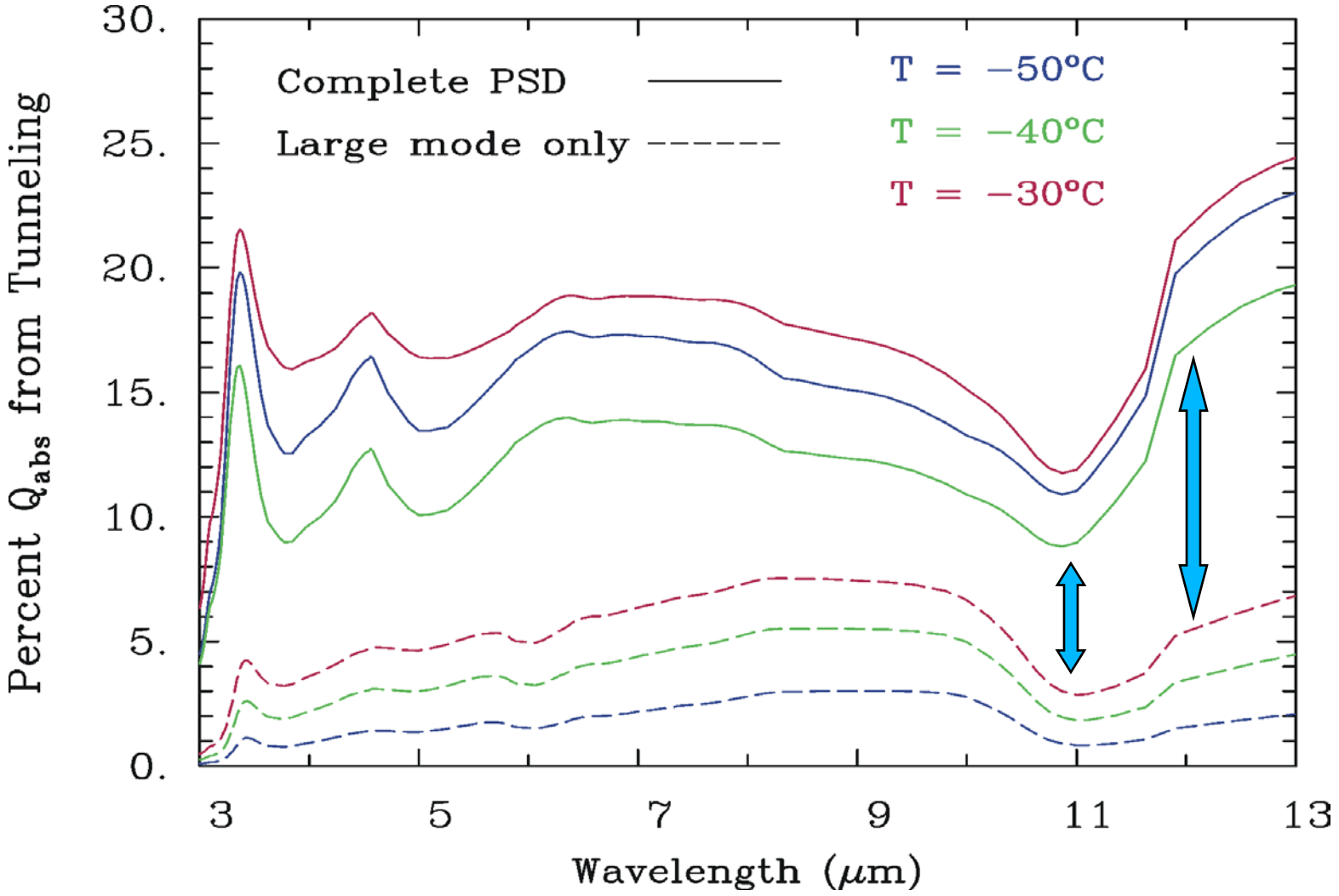

- Satellite remote sensing studies find the 12-to-11 μm absorption optical depth ratio in cirrus to be 1.08 ± 0.04 (Inoue 1985, Parol et al. 1991, Giraud et al. 1997, Giraud et al. 2001)

- Using this ratio and the above principles, an algorithm was designed to make the small ice crystal concentrations in PSD schemes consistent with this ratio.

Comparison of original PSD scheme (dashed) with retrieved PSD (solid)

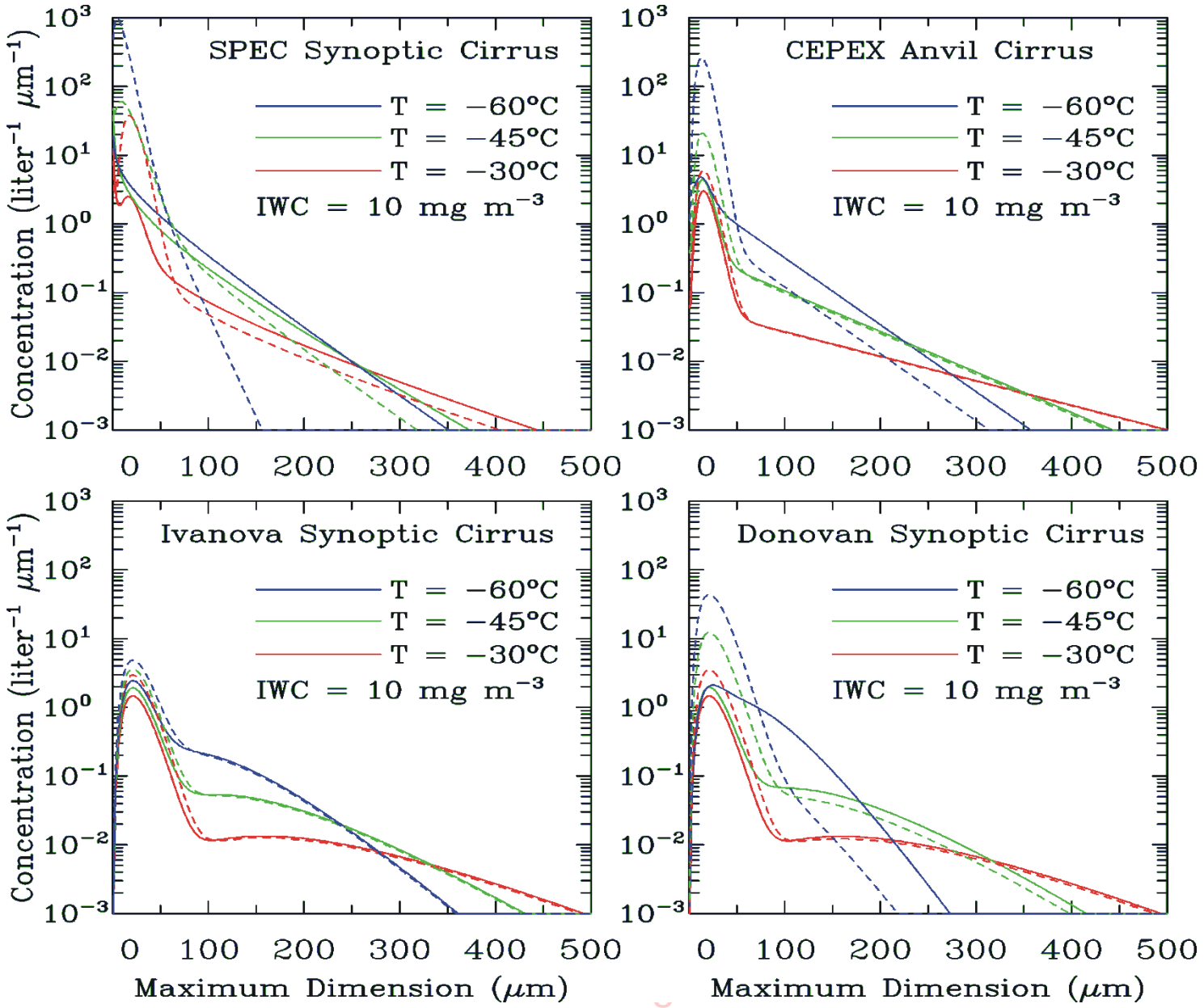

Retrieved PSD having mean and maximum small crystal concentrations

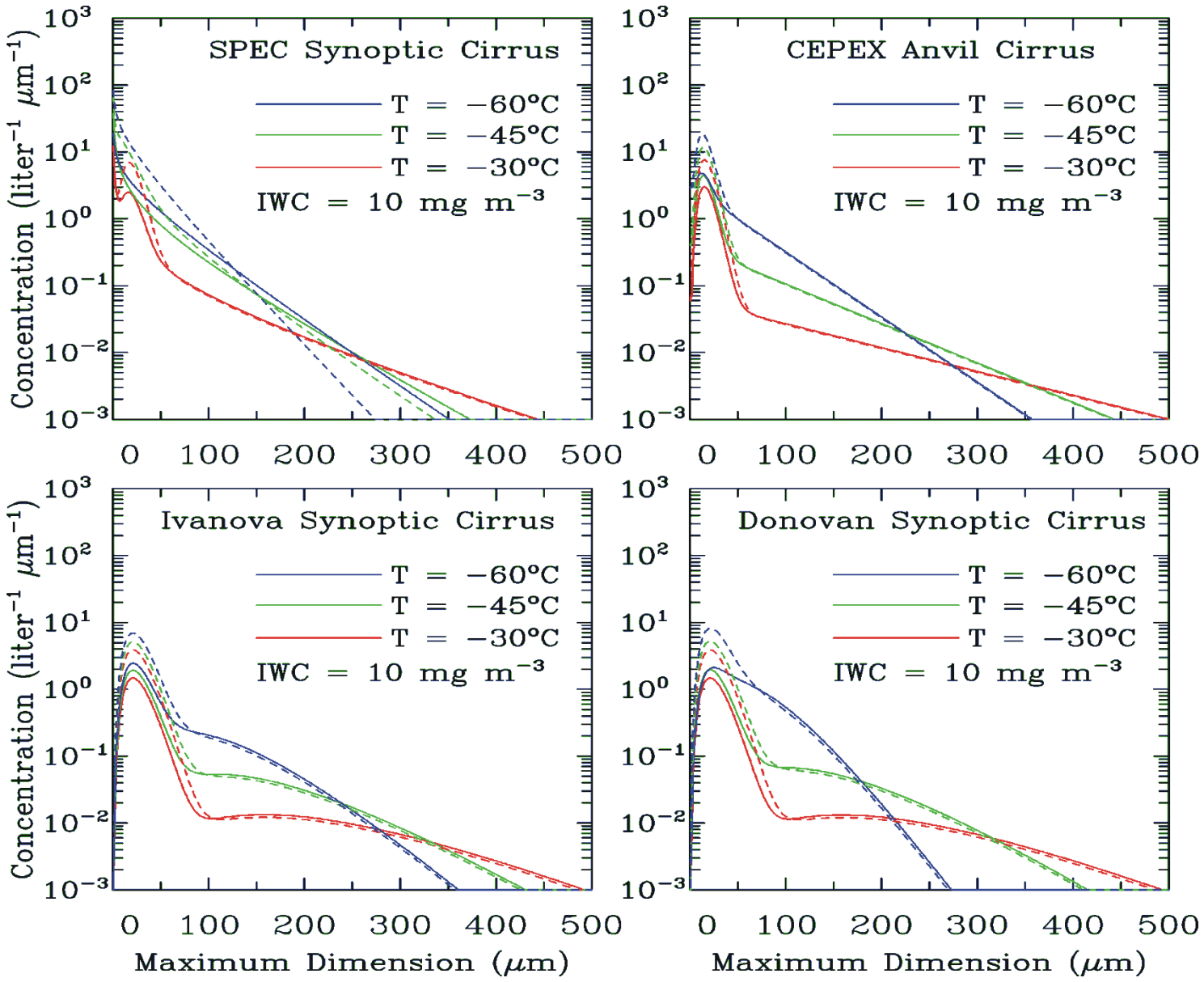

Comparison of CAM Track 5 PSD with PSD schemes having modified small crystal concentrations; T = - 30 ^{o}C

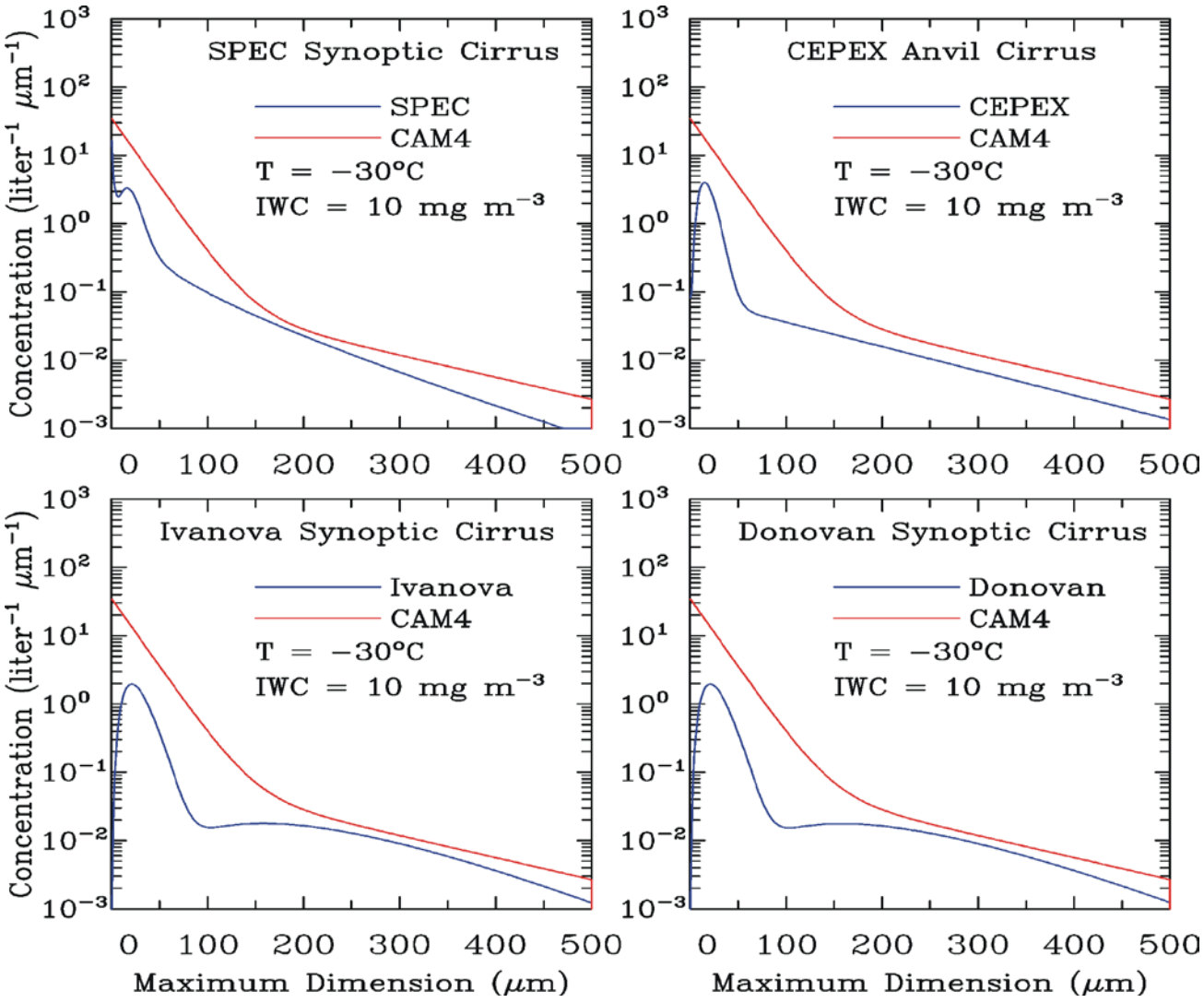

Comparison of CAM Track 5 PSD with PSD schemes having modified small crystal concentrations; T = - 45 ^{o}C

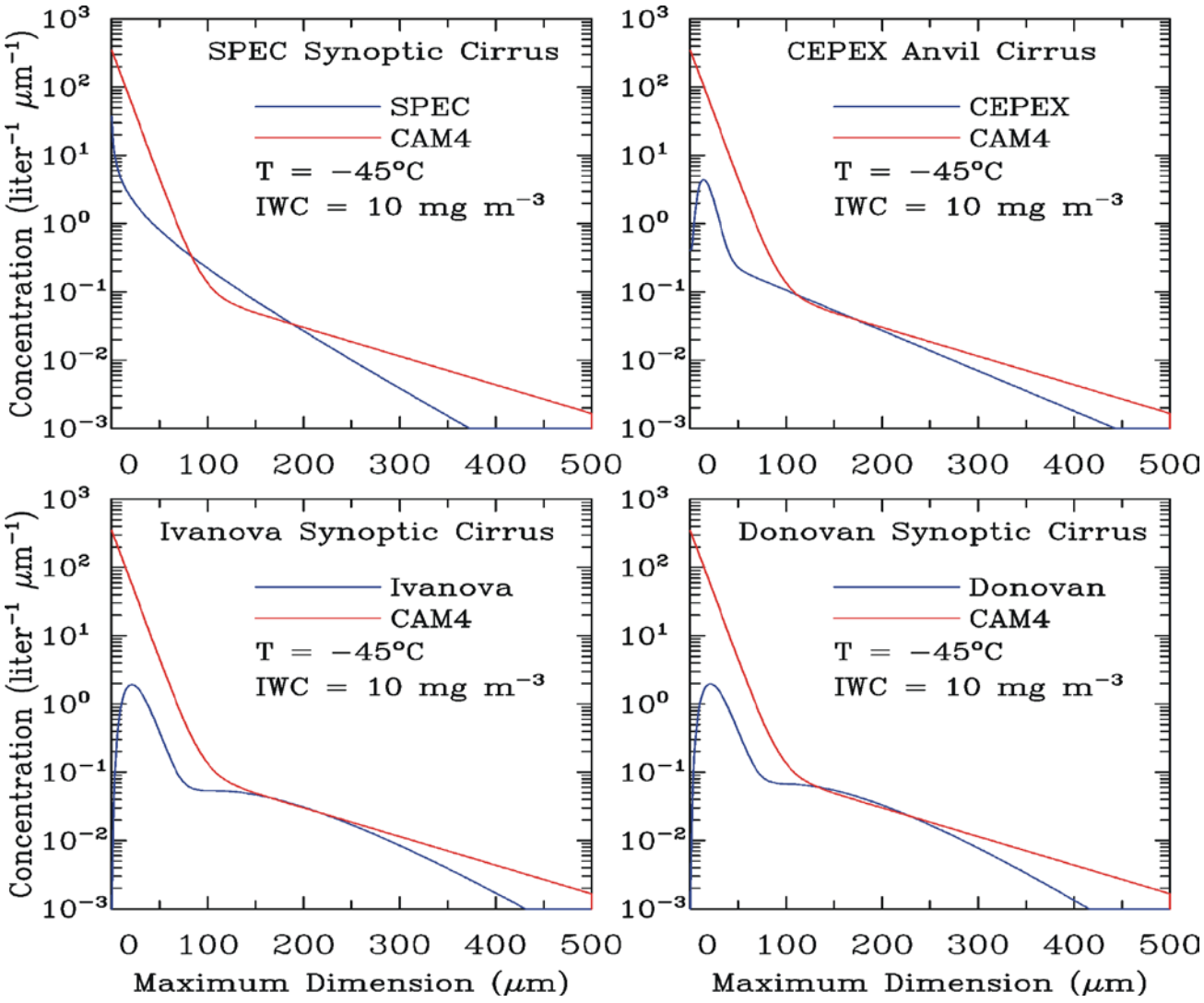

Same as before but now all PSD share the same m-D expression

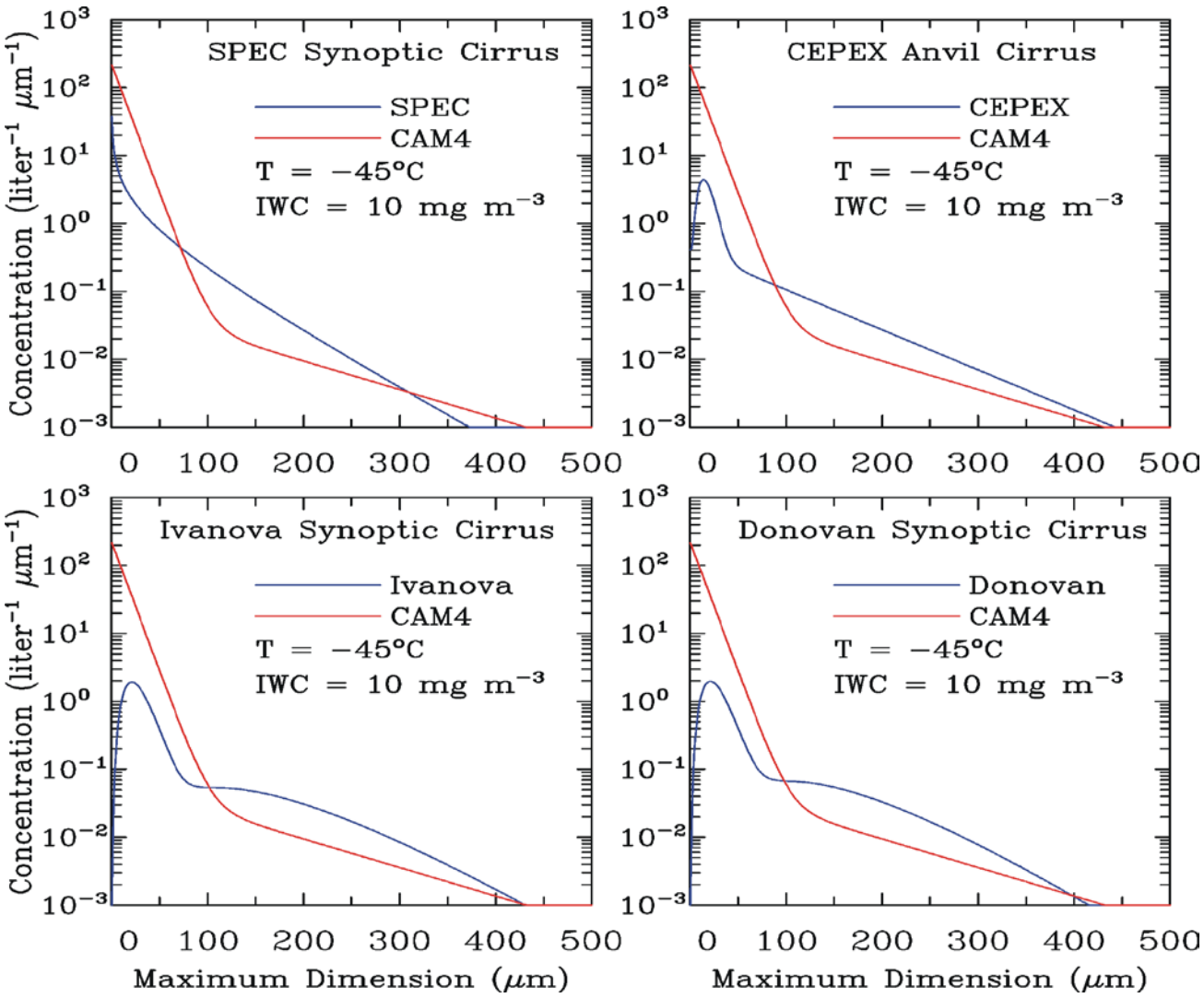

Comparison of CAM Track 5 ice fallspeeds with those from PSD schemes having modified small crystal concentrations

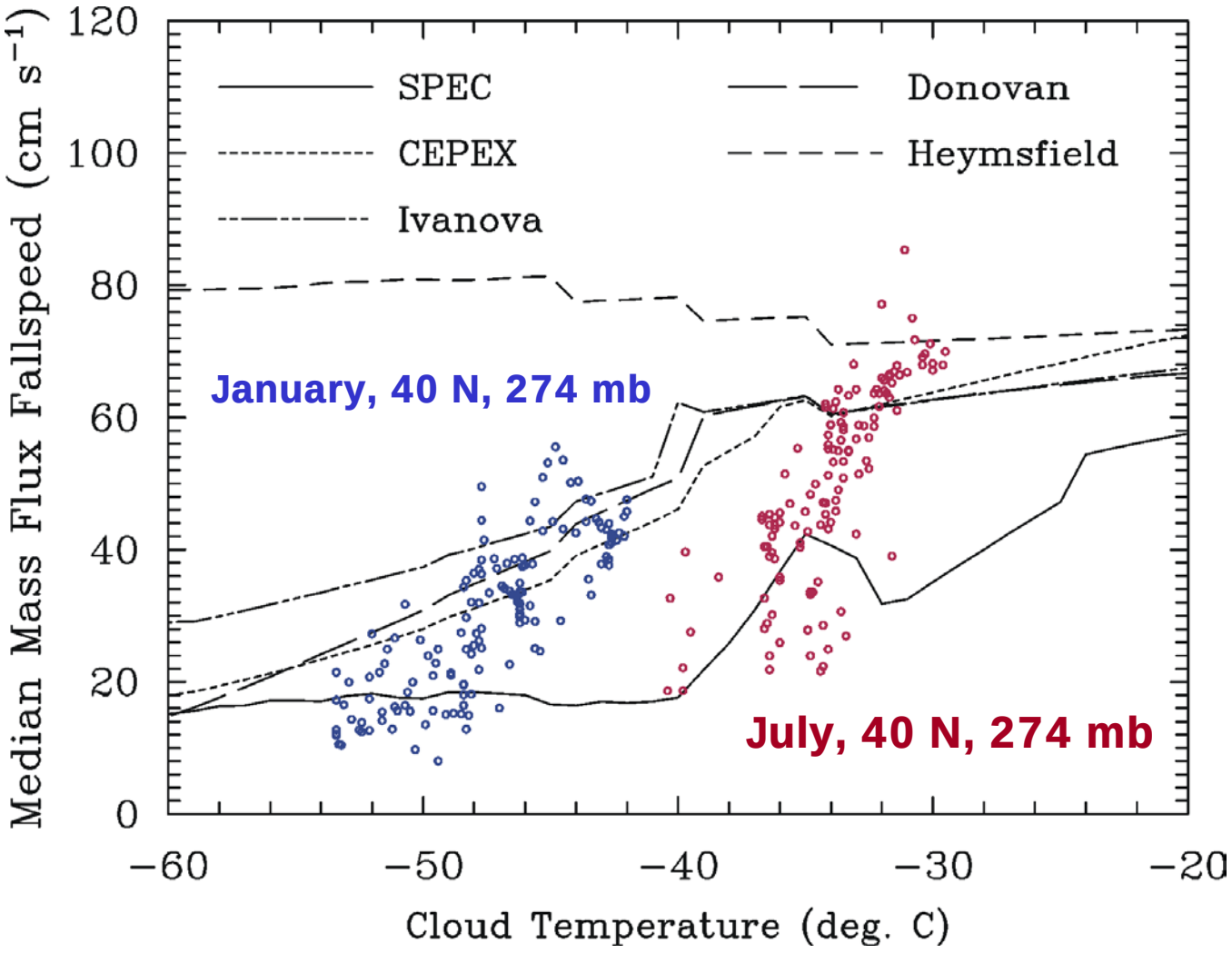

Comparison of CAM Track 5 effective diameters with those from PSD schemes having modified small ice crystal concentrations

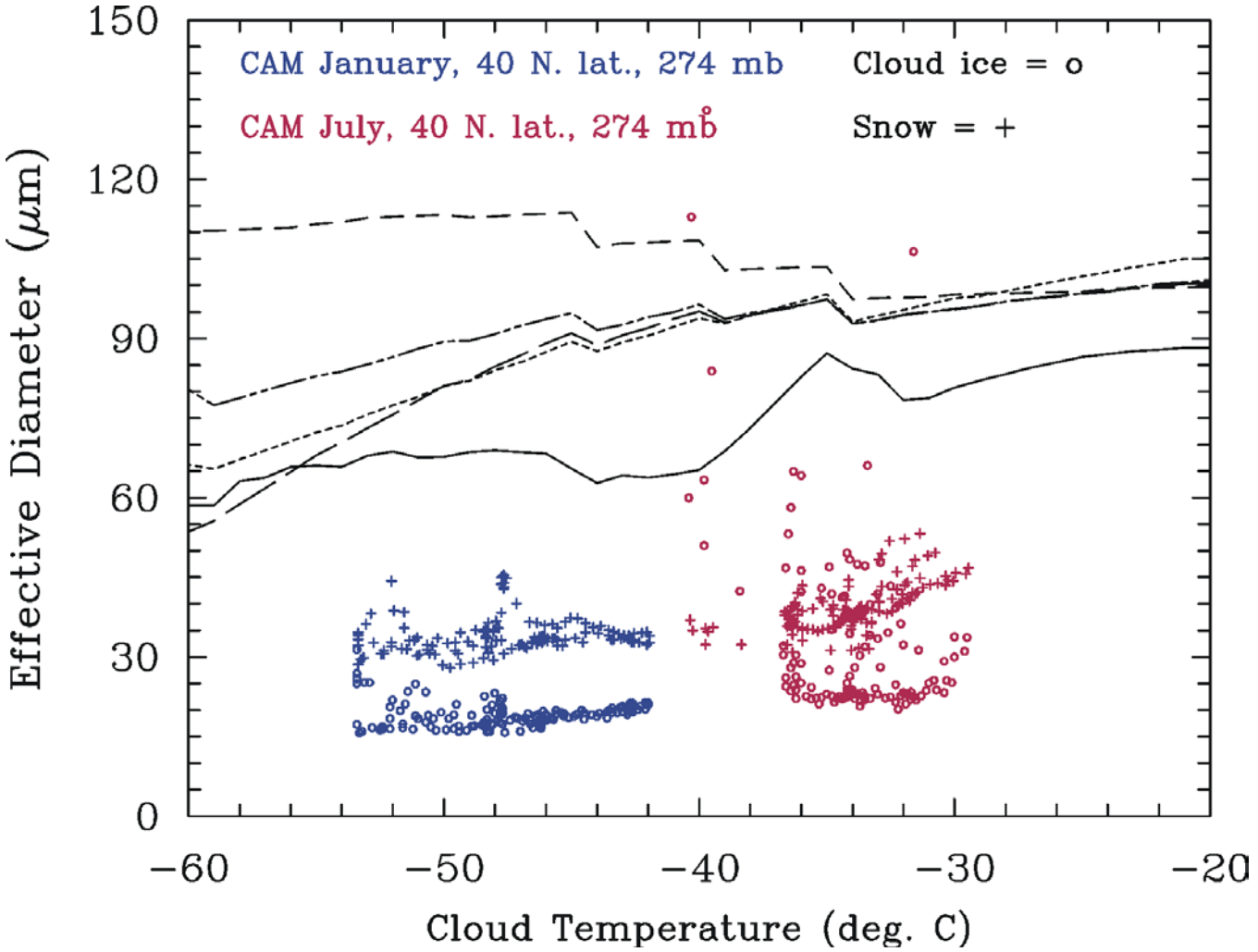

Microphysics Summary for 40 N latitude, 274 mb

	January	July
Data entries	144	132
Mean temperature (^{o}C)	- 47.6	- 34.3
Mean IWC (mg m^{-3})	3.61	7.65
Monthy mean cloud coverage (%)	4.6	6.9
Mean size, cloud ice (microns)	12	21
Mean size, snow (microns)	104	121
Mean number conc., cloud ice (#/liter)	2890	822
Mean number conc., snow (#/liter)	10	13

Summary

1. Cirrus microphysical properties in CAM Track 5 were compared against observations derived from in situ and satellite measurements.

2. CAM PSD exhibit higher N at all sizes, especially small sizes, relative to measurement derived PSD. This is due to (1) lower particle densities and (2) possibly higher ice nucleation rates in CAM.

3. Ice fall velocities in CAM were remarkably consistent with observationally derived V_t. CAM D_e values were ~ 1/3 D_e derived from observations.

4. The temperature dependence of CAM IWCs appear characteristic of those found in nature. Thus for a given IWP, CAM cirrus should be "blacker" than natural cirrus. But LWCF in CAM is too low. This may be due to relatively low cirrus coverage, especially at higher levels.

Wavelength dependence of tunneling

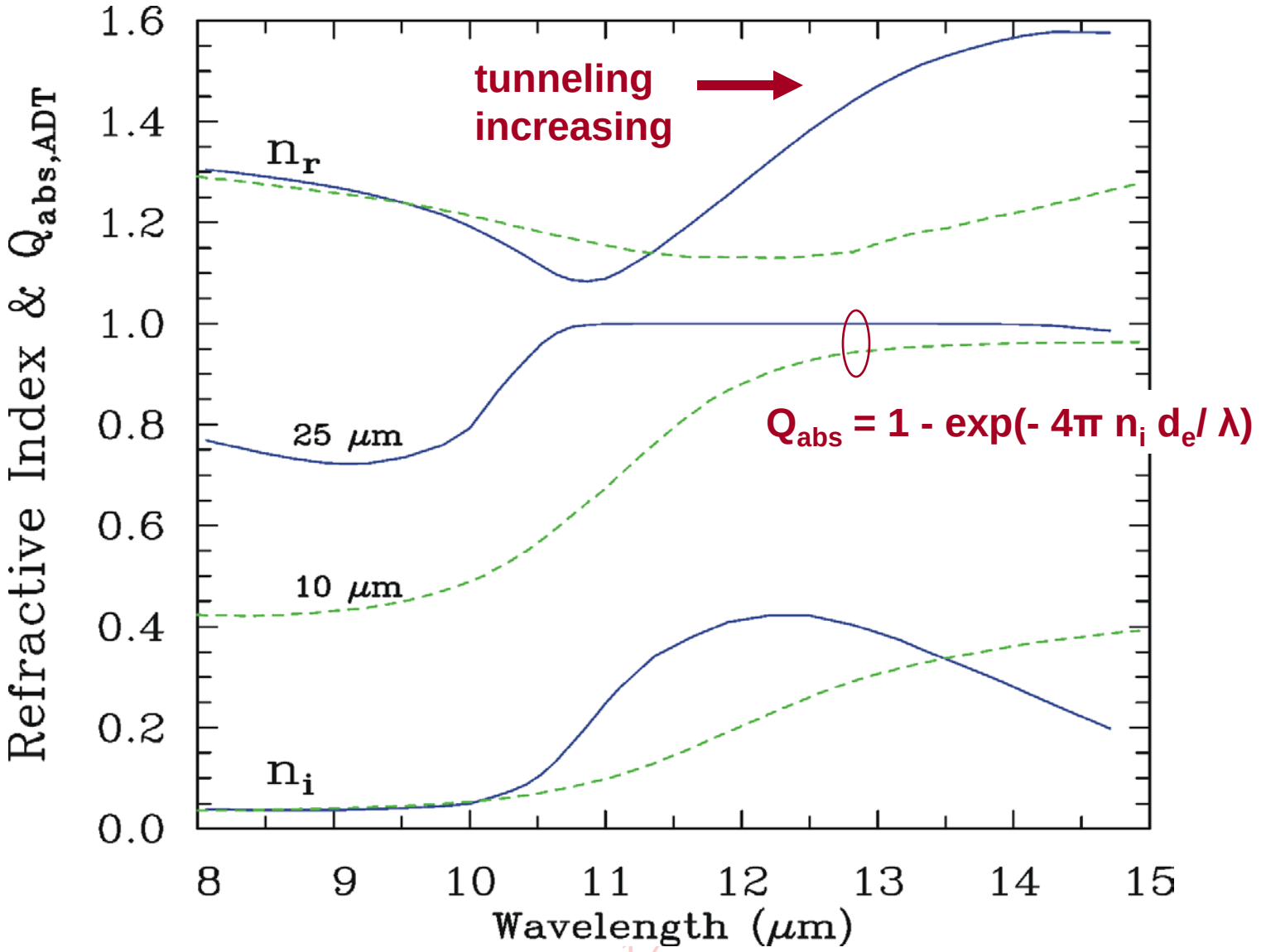

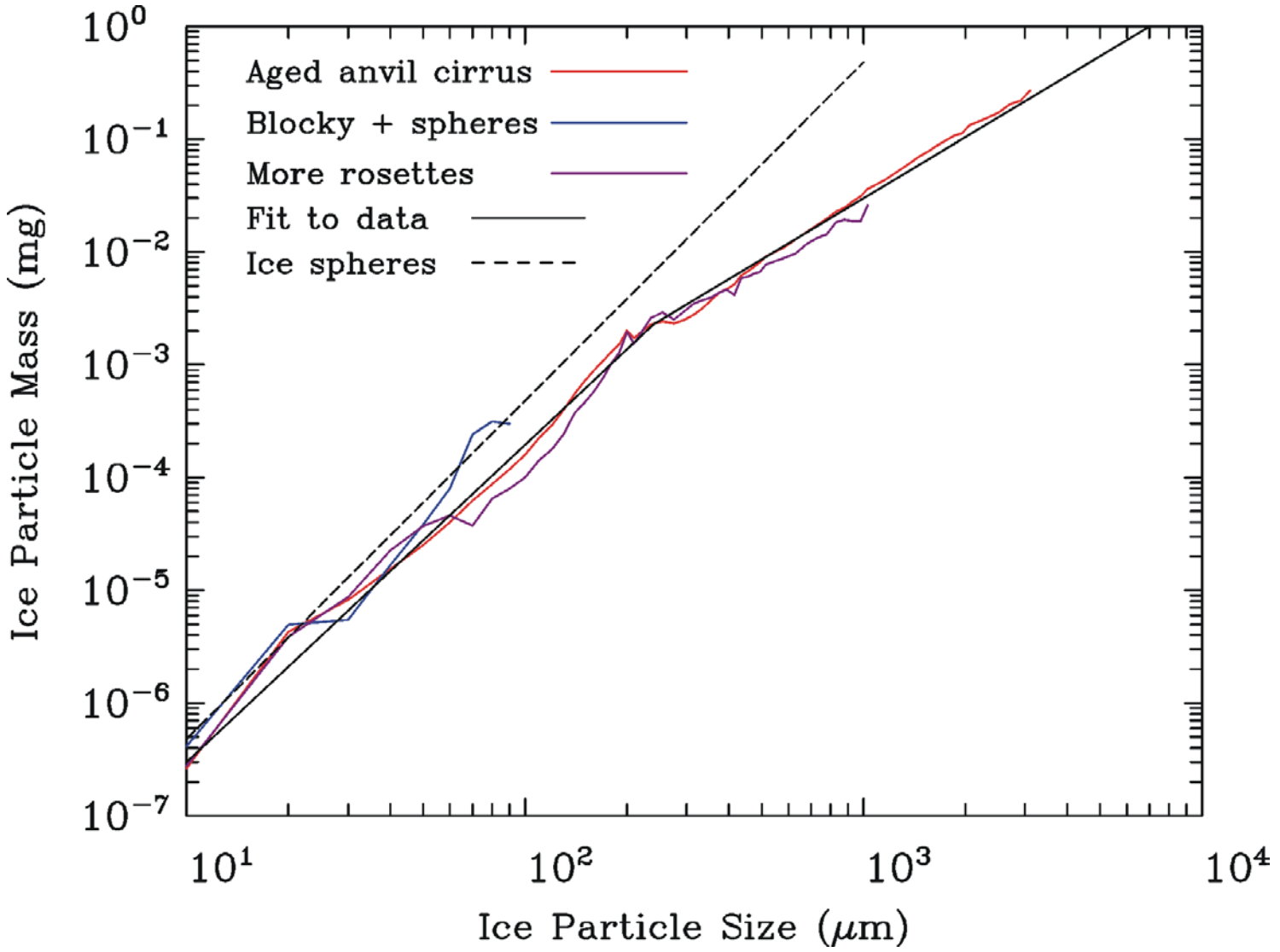
Aged anvil cirrus
Blocky + spheres
More rosettes
Fit to data
Ice spheres
Ice Particle Mass (mg)
Ice Particle Size (μm)
10^0
10^-1
10^-2
10^-3
10^-4
10^-5
10^-6
10^-7
10^1
10^2
10^3
10^4

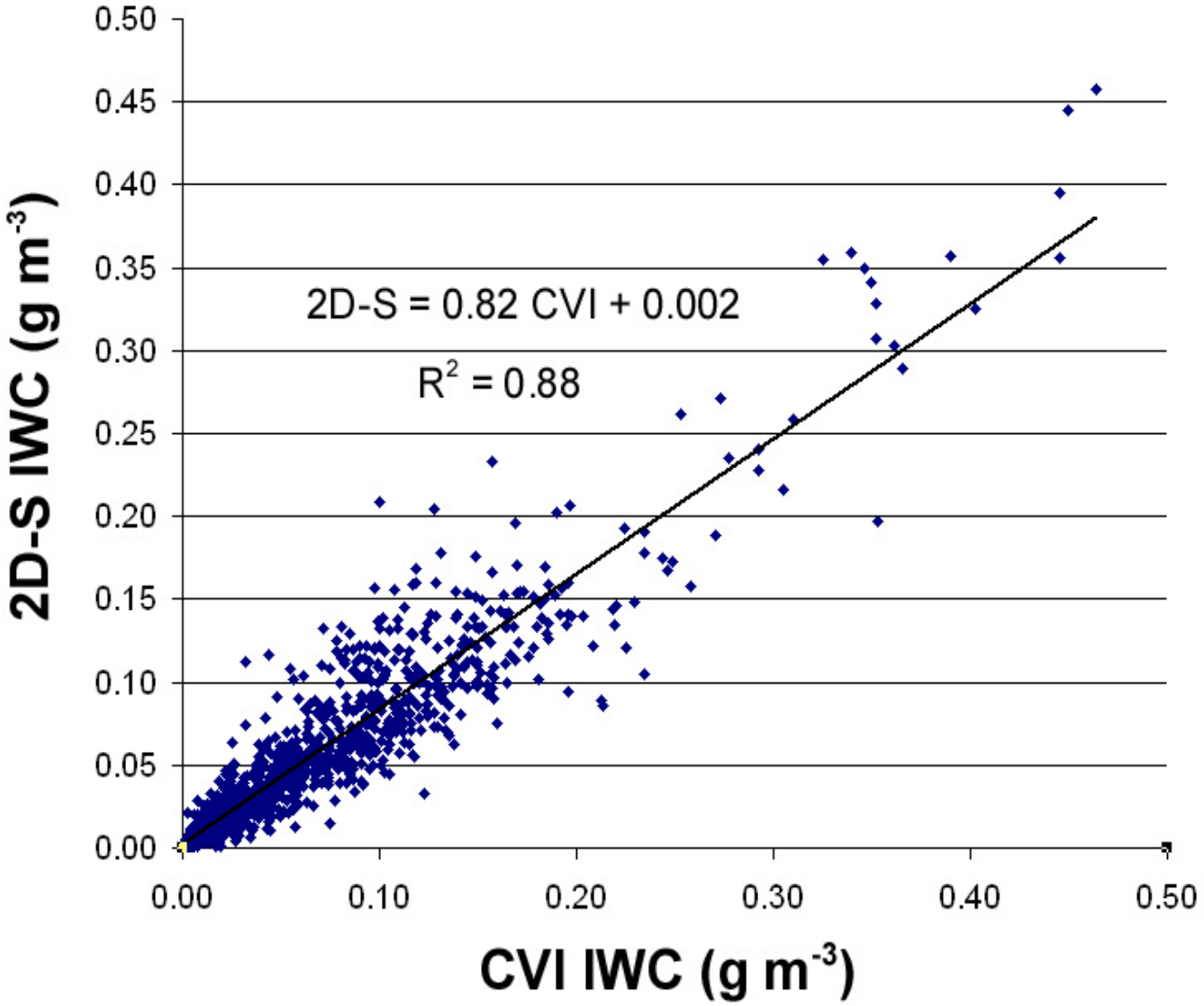
2D-S = 0.82 CVI + 0.002
R2 = 0.88
2D-S IWC (g m-3)
CVI IWC (g m-3)
0.00
0.05
0.10
0.15
0.20
0.25
0.30
0.35
0.40
0.45
0.50

Remote Sensing of Small Ice Crystals (D < 60 μm) and the Process of Photon Tunneling

Tunneling depends on real refractive index, which changes abruptly between 11 and 12 μm wavelength.

Tunneling can account for up to 45% of absorption in ice clouds for terrestrial radiation.

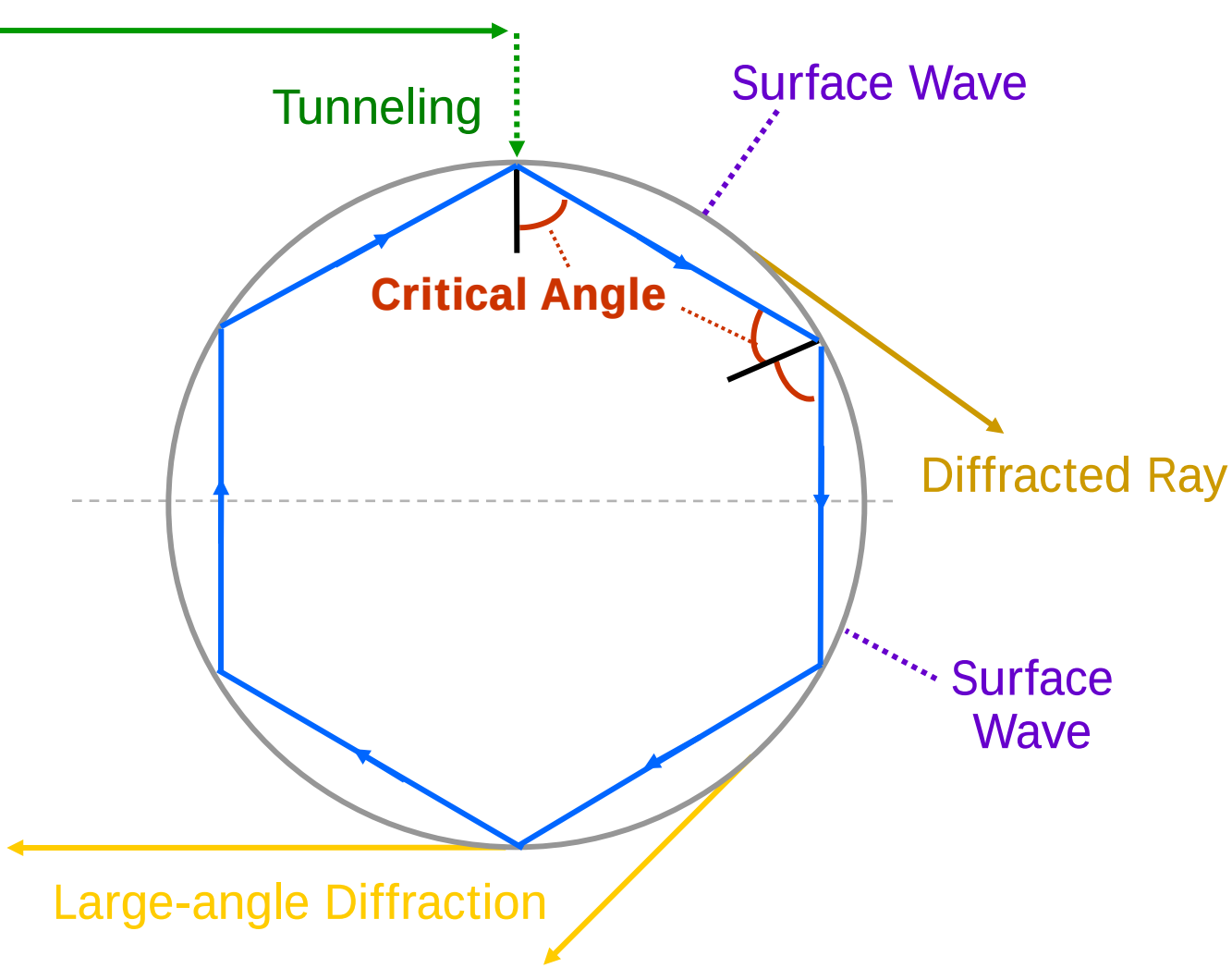

Example of ice particle size distribution (PSD) scheme for evaluating potential tunneling contributions

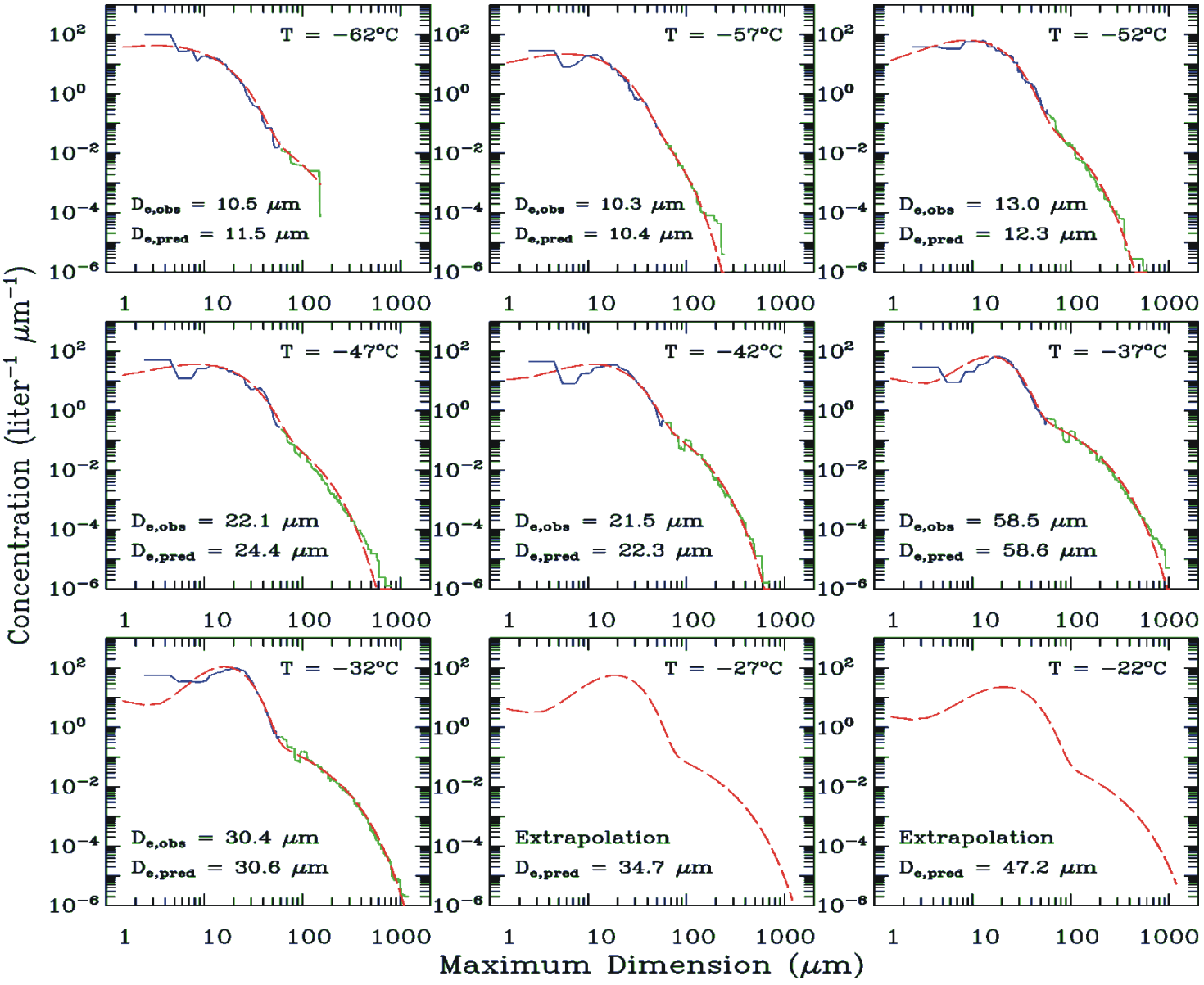

Method for Estimating Small Crystal Concentrations

- using effective emissivities -

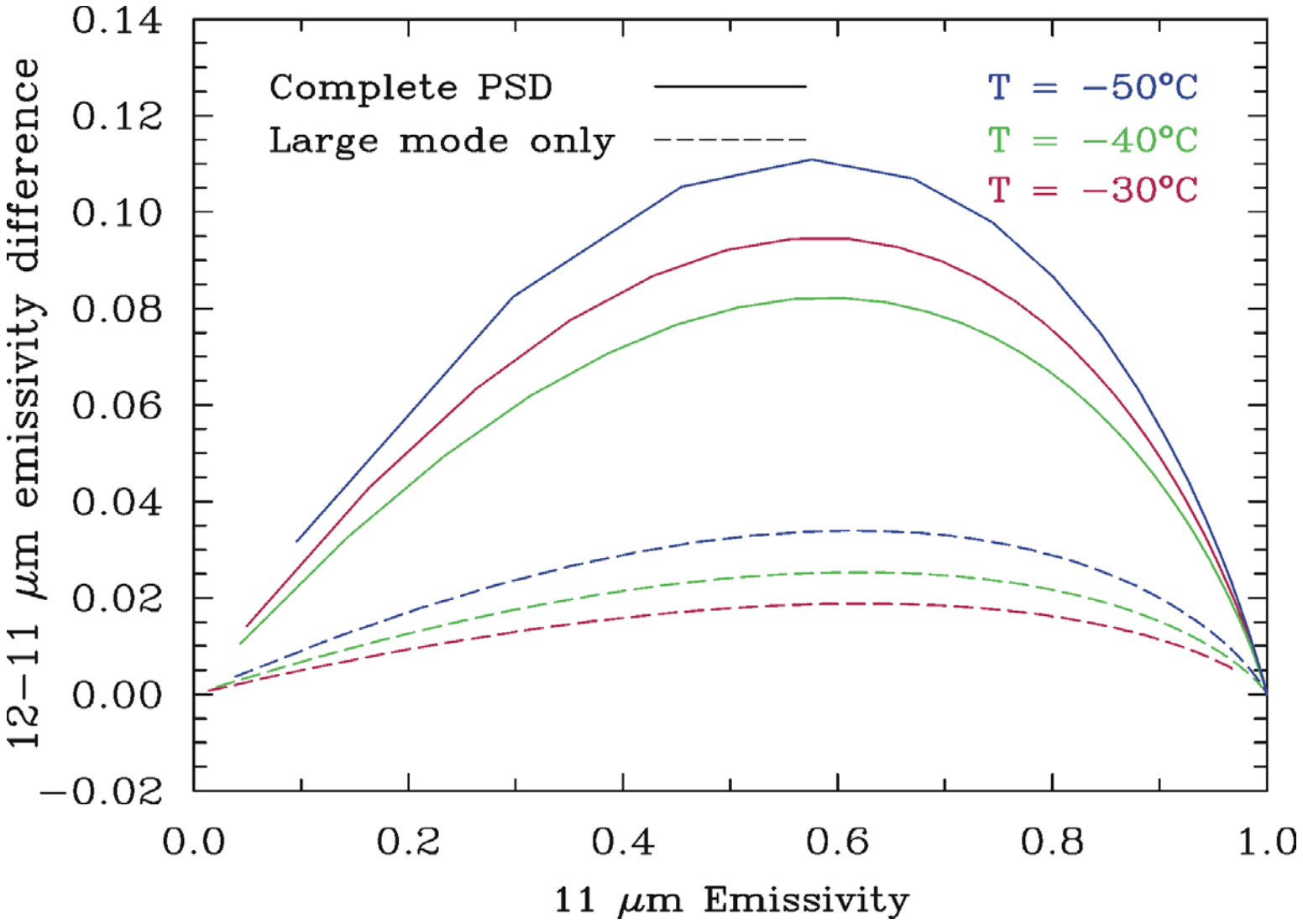

22 July 2007 Case Study: MODIS Retrieval Results

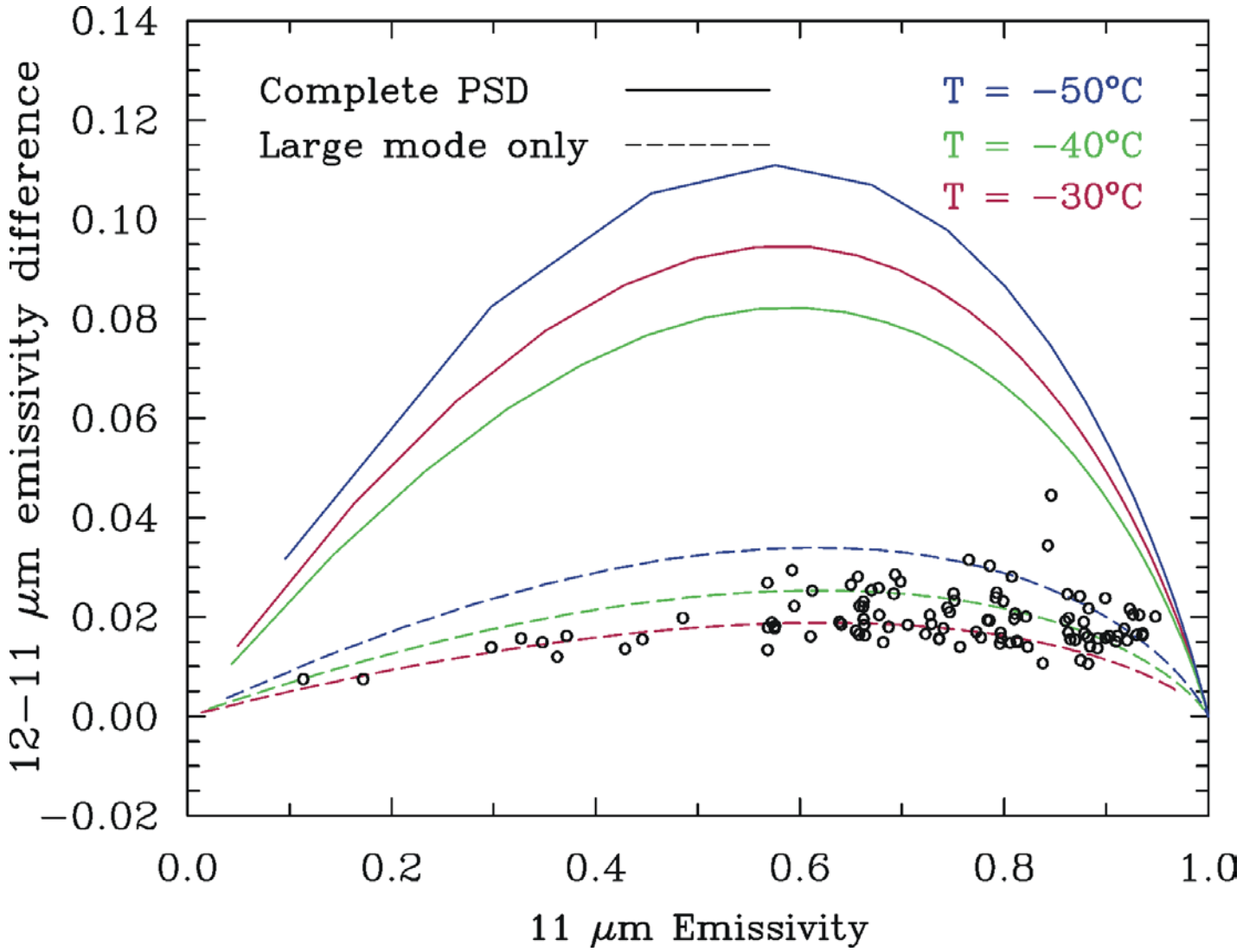

Calculation of ε_{eff} in Retrieval Algorithm

- Based on Parol et al. (1991, JAM) -

Since some scattering may occur, ε retrieved in this way is an effective emissivity, ε_{eff}, which implicitly includes the effects of scattering through its dependence on asymmetry parameter g:

$$\varepsilon_{eff}(12\ \mu m) = 1 - [1 - \varepsilon_{eff}(11\ \mu m)]^{\beta_{eff}}$$

$$\beta_{eff} = Q_{abs,eff(12\ \mu m)}/Q_{abs,eff(11\ \mu m)}$$

$$Q_{abs,eff} = Q_{abs}\ (1 - \omega_o\ g)/(1 - \omega_o)$$

When g => 1, all scattering is completely forward scattering and radiation is not redistributed.

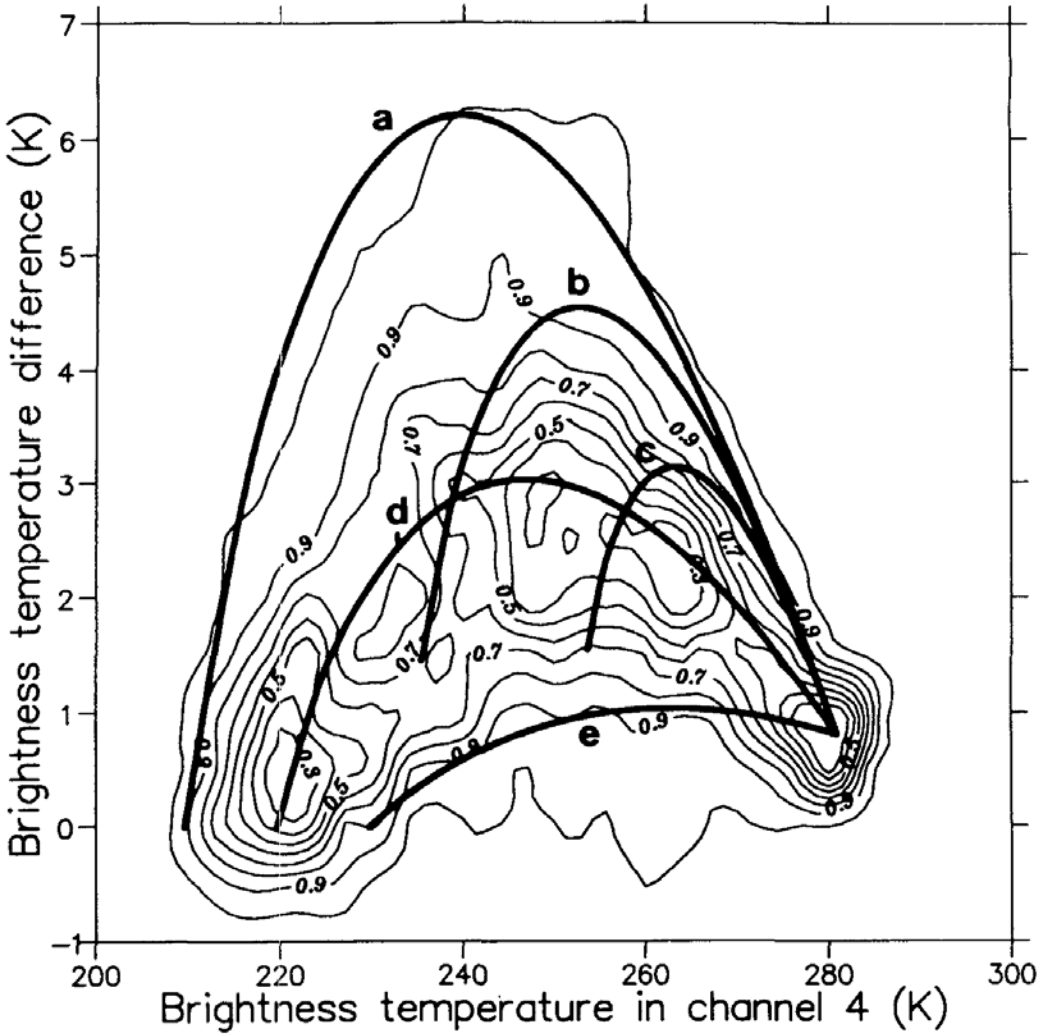

FIG. 2. Comparison between observed (isolines) and theoretical (thick lines) brightness temperature differences $T_4 - T_5$ for the small outlined area in Fig. 1. For example, 70% of the pixels are situated within the isolines 0.7. The thick lines correspond to several combinations of the cloud top temperature T^{cloud}, the cloud cover N, and the absorption coefficient ratio β: (a) T^{cloud} = 210 K, N = 1.00, β = 1.18; (b) T^{cloud} = 210 K, N = 0.75, β = 1.18; (c) T^{cloud} = 210 K, N = 0.50, β = 1.18; (d) T^{cloud} = 220 K, N = 1.00, β = 1.08; (e) T^{cloud} = 230 K, N = 1.00, β = 1.00. The cloud-free brightness temperatures is fixed to 281.0 and 280.2 K in channels 4 and 5, respectively.

Probability densities of 11-12 μm BTD vs. 11 μm brightness temperature. Curve D describes the average relationship found by Inoue (1985), where β_{eff} = 1.08.

Figure from Parol et al. (1991, JAM).

Maximum Estimate of β_{eff} vs. Cloud Temperature From Giraud et al., 1997 J. Applied Meteorology

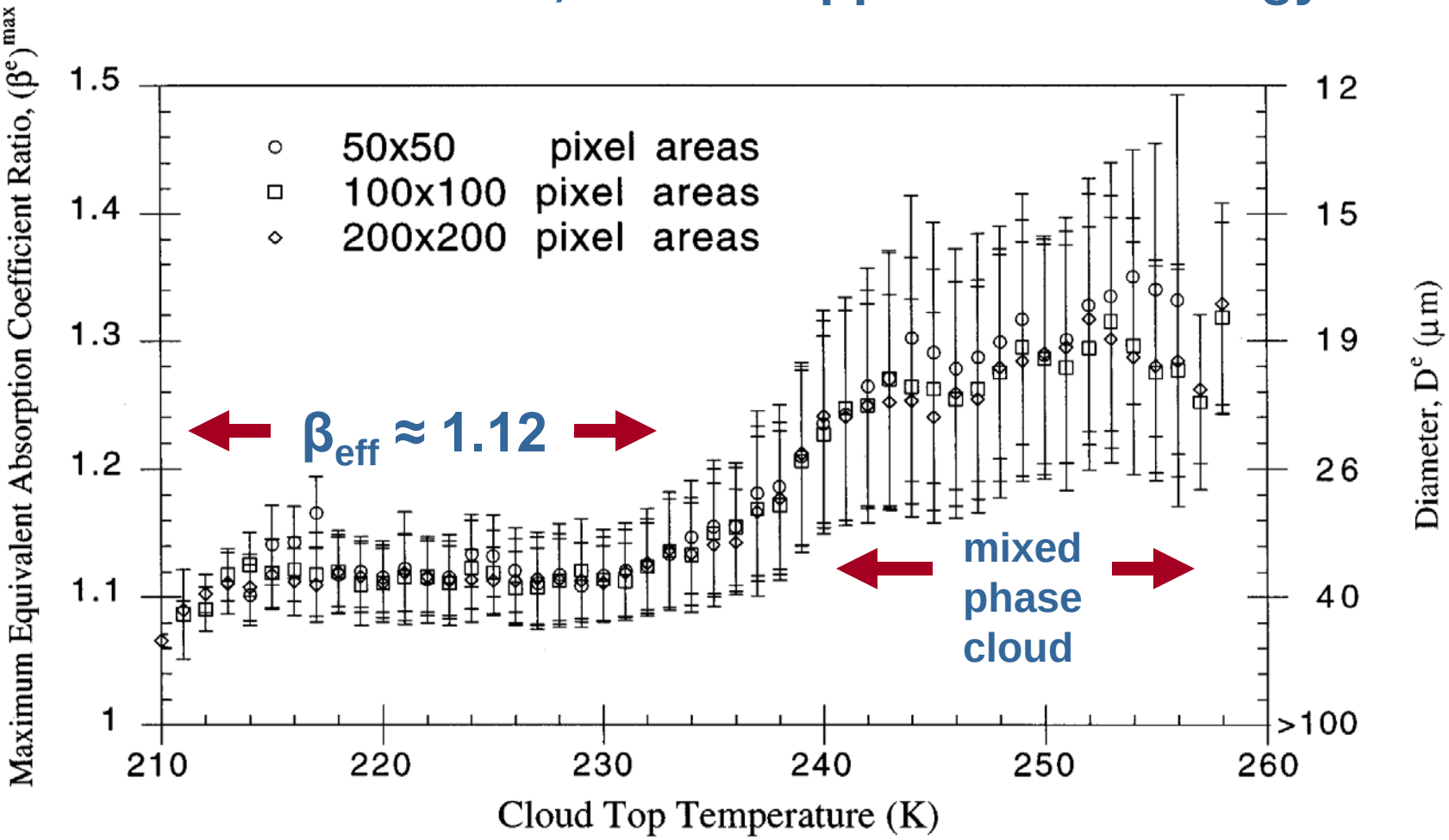

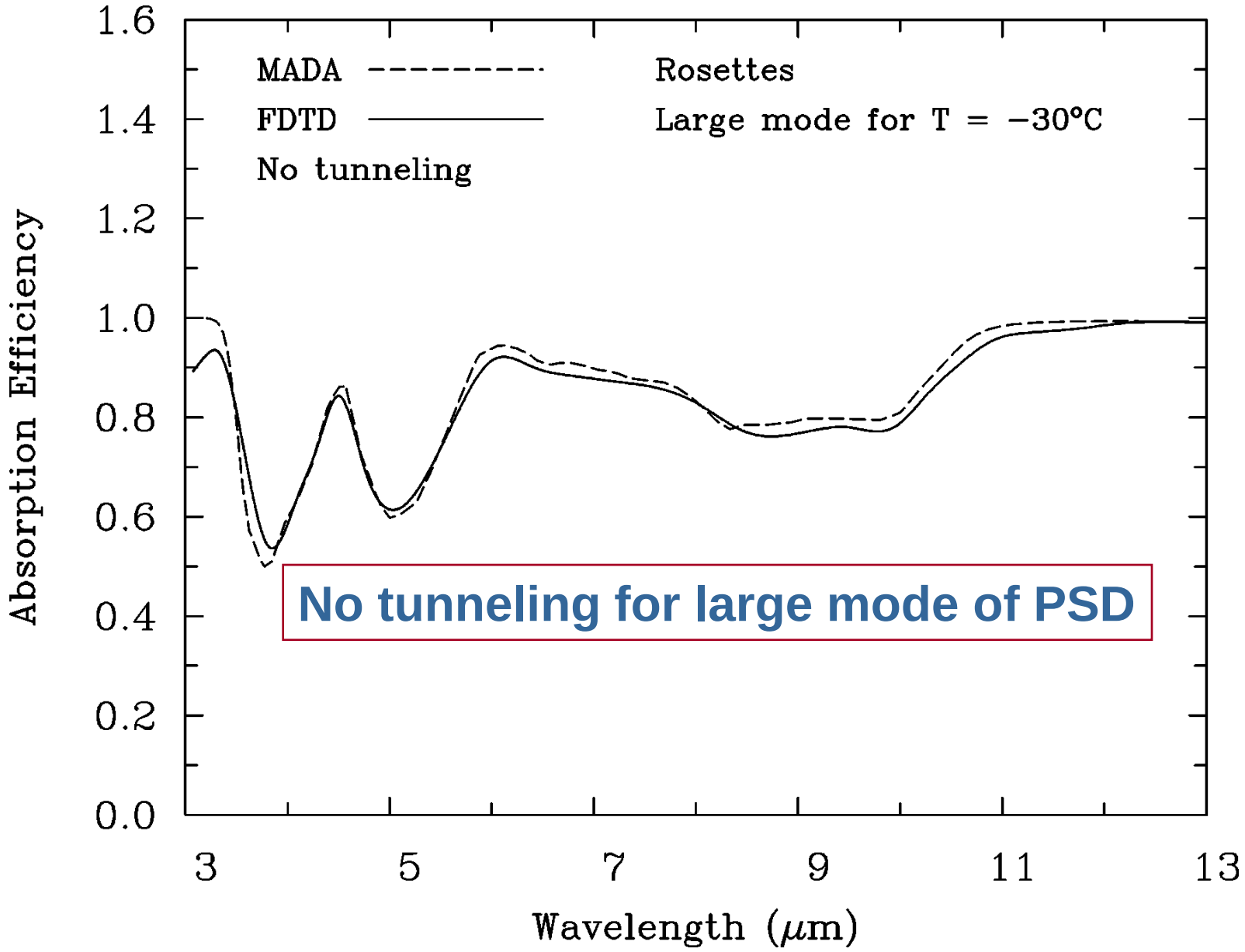

No tunneling for large mode of PSD

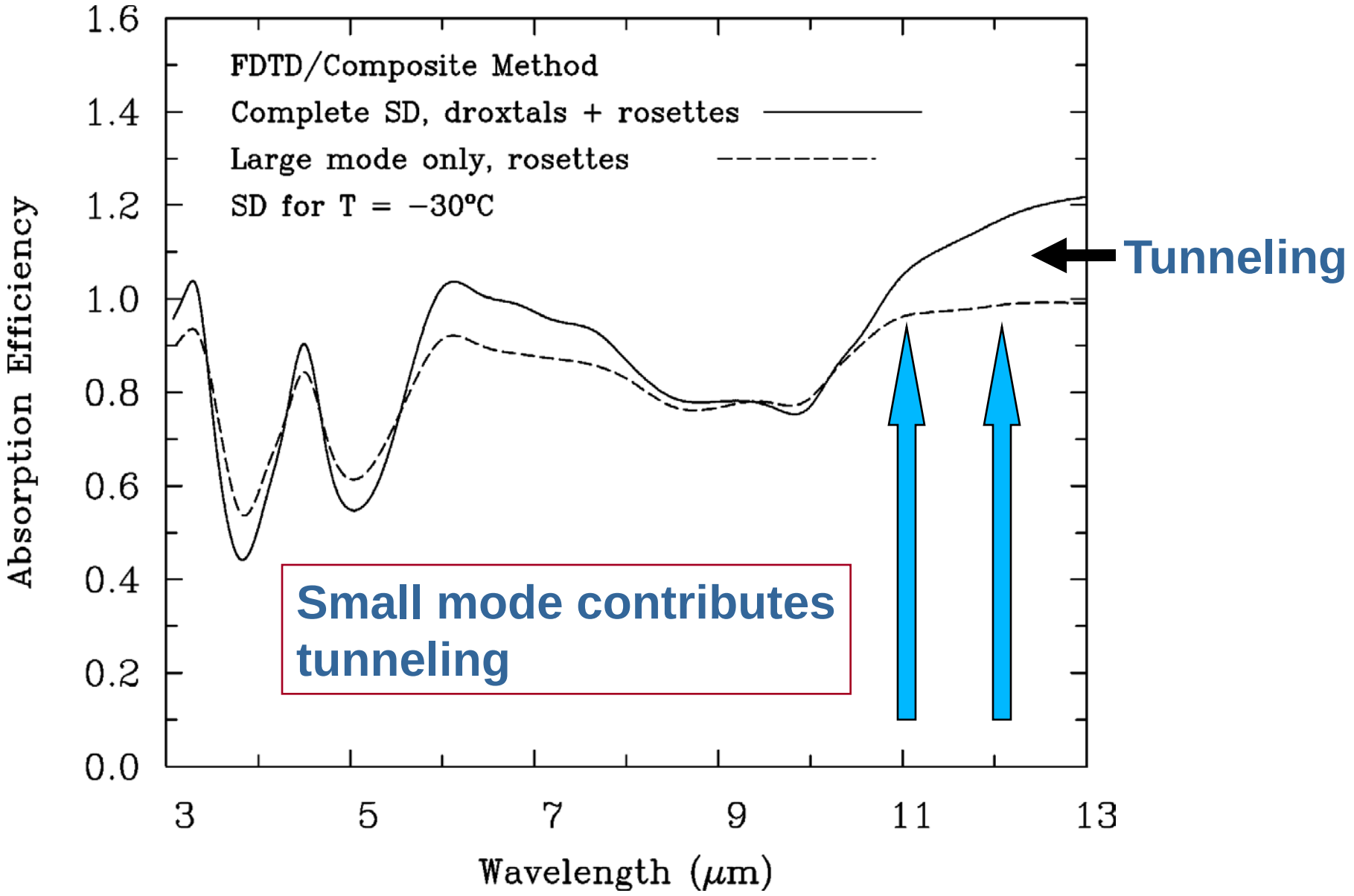
FDTD/Composite Method
Complete SD, droxtals + rosettes
Large mode only, rosettes
SD for T = −30°C
Absorption Efficiency
Wavelength (μm)
1.6
1.4
1.2
1.0
0.8
0.6
0.4
0.2
0.0
3
5
7
9
11
13
Tunneling
Small mode contributes tunneling

Cloud Optical Properties Depend on the Ice Crystal Mass- and Projected Area-Dimension Relationships That Characterize the PSD

1. Mass = $m = \alpha D^{\beta}$
2. Projected area = $P = \gamma D^{\sigma}$

Constants giving P & m = function of temperature for mid-latitude cirrus. Based on 22 cirrus flight missions, 104 horizontal legs and 15,000 km of in-cloud sampling, and Heymsfield et al. (2007).

Method for Estimating Small Crystal Amounts

1. Begin with satellite retrievals of cloud temperature and emissivity (ε) at 11 and 12 μm wavelength channels.

2. Use the retrieved cloud temperature to estimate the PSD mean size $\overline{D}$ and dispersion (ν) for large and small mode. Difference between the solid and dashed curves results primarily from differences in the contribution of the PSD small mode to the IWC. This also determines effective diameter, D_e. Note that the large mode $\overline{D}$ and ν have little effect on above curves.

3. Locate the retreived Δε and the ε(11 μm) by (1) incrementing the modeled IWP to increase ε(11 μm) and (2) incrementing the small mode IWC, which elevates the curve.

4. If all IWC is in the small mode and retrieved Δε and ε(11 μm) is still not located, then decrease small mode $\overline{D}$ to locate them.

Method for Estimating Small Crystal Amounts - continued -

5. If the retrieved point lies below the "large mode only" curve (e.g. a dashed curve), then systematically decrease $\overline{D}$ for large mode until a match is obtained. Negative $\Delta\varepsilon$ values correspond to maximum allowed large mode $\overline{D}$ values.

6. This methodology retrieves IWP, D_e, the small-to-large mode ice crystal concentration ratio, and the ice particle concentration for a given IWC. It also estimates the complete PSD (even when it is bimodal).

Tunneling Efficiencies for Different Crystal Shapes

(from Mitchell et al. 2006, JAS)

CRYSTAL SHAPE	TUNNELING EFFICIENCIES		
	Small Mode of SD	Large Mode Mean of SD .	
	D = 14 to 20 μm	D = 53 μm	D = 170 μm
Aggregate	0.35	0.30	0.15
Bullet Rosette	0.70	0.40	0.15
Hex. Column	0.90	0.65	0.40
Hollow Column	0.70	0.50	0.15
Hex. Plate	0.60	0.15	0.00
Droxtal	1.00	0.80	0.40

Red circles indicate typical crystal shapes found in the small or large mode.
Efficiencies are one reason tunneling is mostly manifested in the small mode.

Sensitivity to different microphysical assumptions

Bimodal w CEPEX PSD - std crystal shapes

Monomodal - std crystal shapes

Bimodal – Planar polycrystals

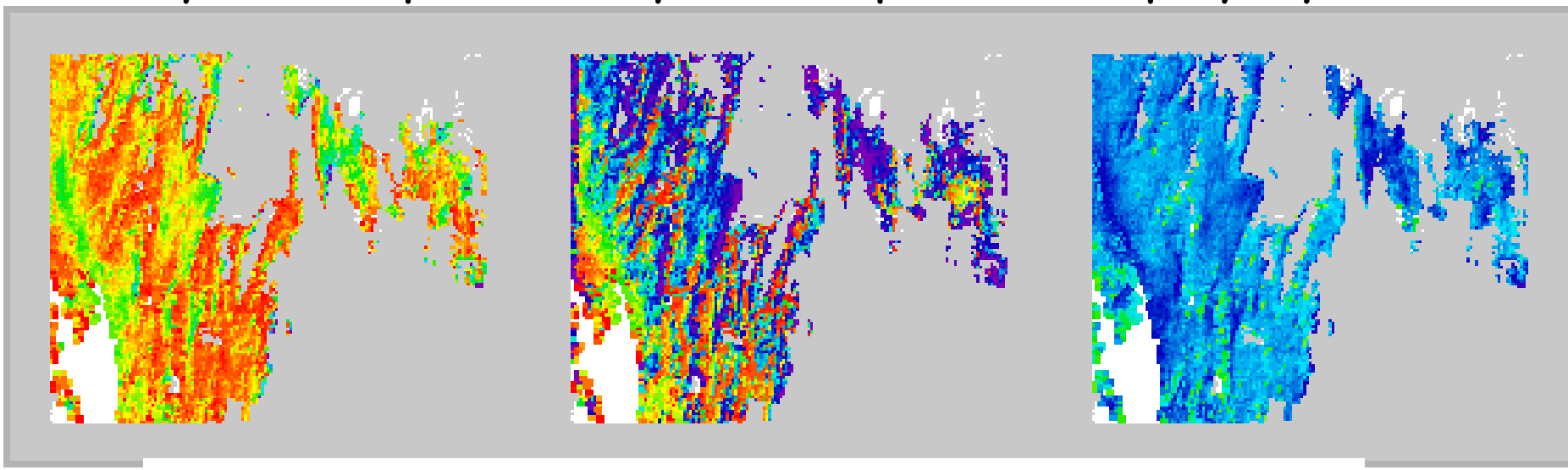

2643 60 78 96 113 130

Effective Diameter D_{EFF} (μm)

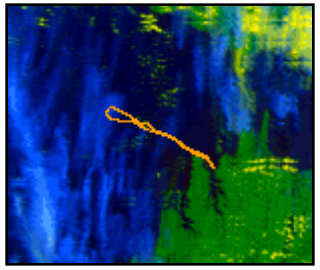

0.47 0.86 11.03-μm Composite

Sensitivity to different microphysical assumptions

Bimodal w CEPEX PSD - std. crystal shapes

Monomodal – std. crystal shapes

Bimodal - Planar polycrystals

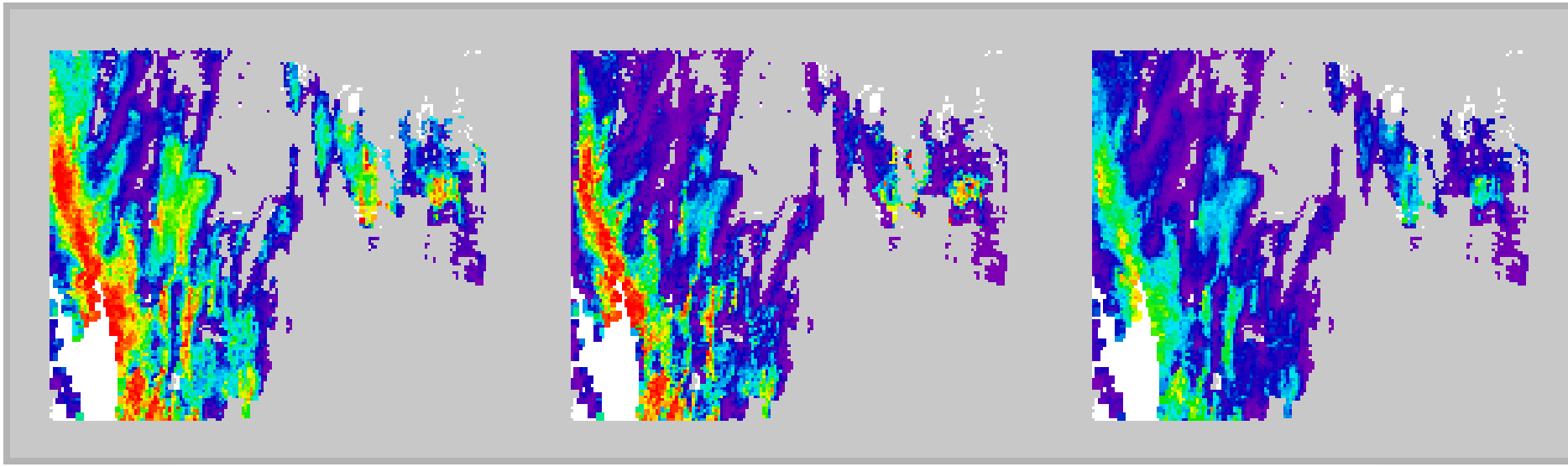

0 15 30 45 60 75 90

Ice-water path (g/m^2)

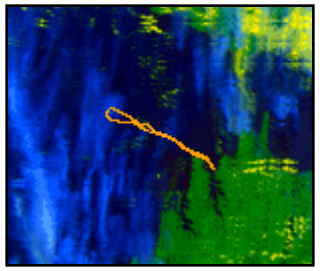

0.47 0.86 11.03-μm Composite

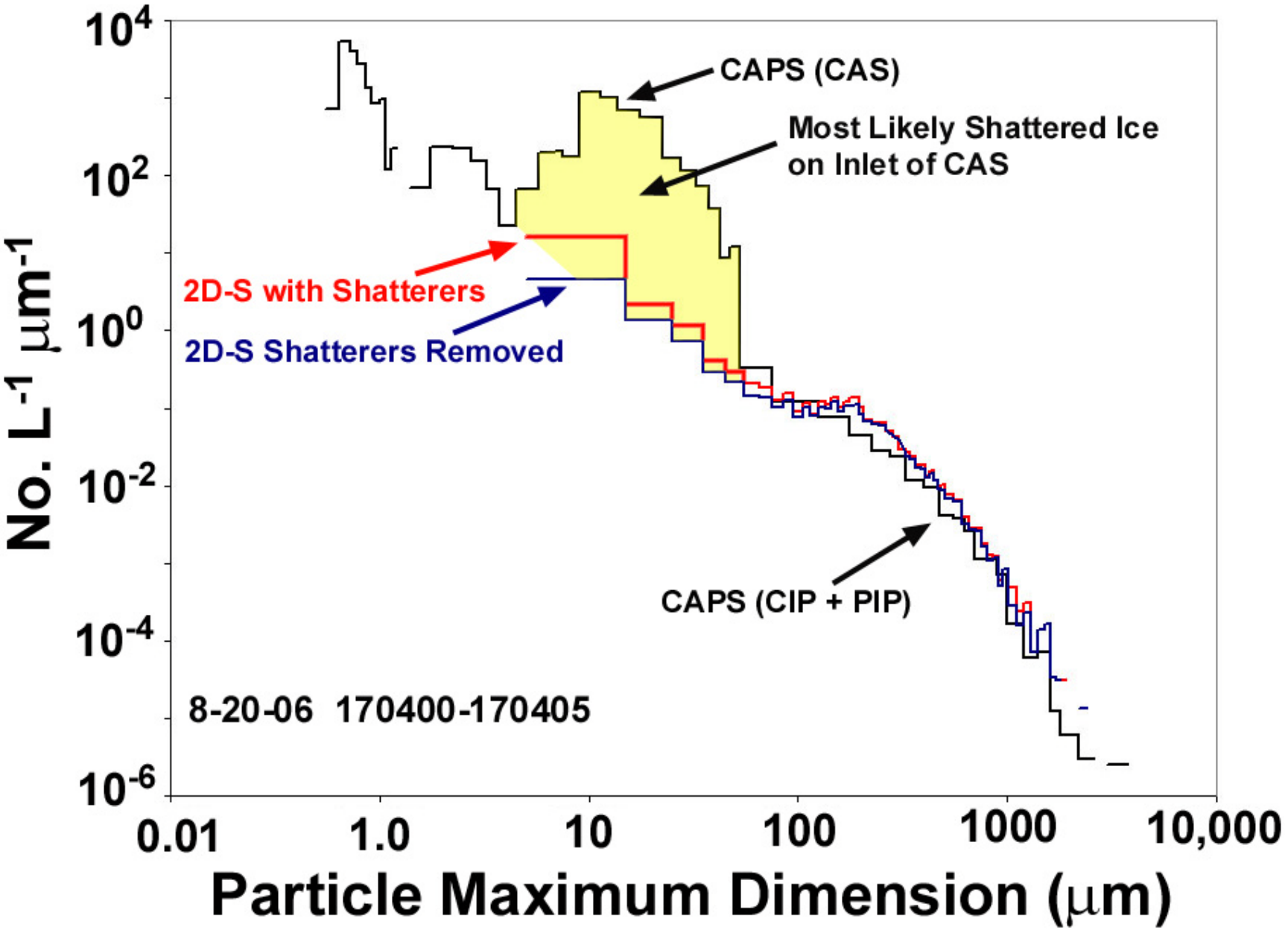
CAPS (CAS)
Most Likely Shattered Ice on Inlet of CAS
2D-S with Shatterers
2D-S Shatterers Removed
CAPS (CIP + PIP)
8-20-06 170400-170405
No. L-1 μm-1
Particle Maximum Dimension (μm)
10^4
10^2
10^0
10^-2
10^-4
10^-6
0.01
1.0
10
100
1000
10,000